Magnetic ordering and phase transitions in planar antiferromagnetic systems with a Kagomé lattice

R. S. Gekht*) and I. N. Bondarenko

L. V. Kirenskiĭ Institute of Physics, Siberian Branch of the Russian Academy of Sciences, 660036 Krasnoyarsk, Russia

(Submitted 28 August 1997)
Zh. Éksp. Teor. Fiz. **113**, 2209–2220 (June 1998)

We study the process of magnetic ordering in planar antiferromagnetic systems with a Kagomé lattice. It is found that if the interaction between next-nearest-neighbor spins is taken into account, the heat capacity of such systems has a singularity at a finite temperature T. On the basis of a scaling analysis of finite-size systems we study the behavior of thermodynamic quantities in the neighborhood of a phase transition. We find that the phase transition at the critical point is due to discrete- and continuous-symmetry breaking, in which the long-range chiral order and the power-law translational spin order emerge simultaneously. Finally, we calculate the temperatures of the transition to different (with three and nine spins per unit cell) ordered states. © *1998 American Institute of Physics.* [S1063-7761(98)02106-4]

1. INTRODUCTION

Lately there has been an upsurge of interest in phase transitions in the low-temperature range in compounds with a Kagomé lattice. Because of the special geometry of the lattice (triangles in a layer alternate with hexagons), the spin systems are highly frustrated. As the temperature drops, the ordering proceeds much more slowly in comparison to ordinary frustrated systems. It is known[1,2] that this situation occurs because in systems with a coordination number much smaller than, say, in triangular antiferromagnets, at large values of S in addition to states with nontrivial global degeneracy there can be local degenerate states. As a result, when there is interaction between the nearest-neighbor spins, there is no single finite temperature at which a phase transition to a magnetically ordered state can occur. The additional interaction between next-nearest-neighbor spins partially lifts the degeneracy and may lead to a phase transition at finite temperatures.[3] Nevertheless, since the frustration effects are still present, the process of ordering and stabilization of structure is slower than in nonfrustrated systems.

Ising systems with a Kagomé lattice have been studied fairly recently. As in Ising systems with a triangular lattice, in the classical ground state the entropy per spin is finite (interaction of nearest neighbors), but the decrease in the spin–spin correlation functions at $T=0$ follows an exponential law rather than a power law (superfrustrated systems[4,5]). Heisenberg systems with a Kagomé lattice were under intensive study at the beginning of the 1990s. The excitations of such systems have a null spectrum in the entire magnetic Brillouin zone.[6] Quantum[7] and thermal[2,3] fluctuations lift the degeneracy and select states with a planar spin configuration. XY systems have not been studied so thoroughly. It is known that as $T\to 0$, the spins in such systems are less ordered than in Heisenberg systems. Here the correlation function of an XY system is similar to the correlation function of the three-state Potts model[8] $(T\to 0)$, while the correlation length of Heisenberg systems diverges in the zero-temperature limit.[2,8]

In the $MFe_3(OH)_6(SO_4)_2$ family of compounds (M=H_3O, Na, K, Rb, Ag, NH_4, Tl, Pb, and Hg) called jarosites (the name has its origin in mineralogy) and in their chromium analog $KFe_3(OH)_6(CrO_4)_2$, the magnetic iron ions Fe^{3+} form a Kagomé lattice in the c plane.[9–11] The crystalline structure of such compounds is hexagonal (the space group is $R\bar{3}m$). According to the experimental data, the interactions between nearest-neighbor spins inside a layer and between layers is antiferromagnetic.[12] Neutron-diffraction, Mössbauer, and other measurements involving jarosites show that in jarosites at low temperatures magnetic ordering can be accompanied by formation of triangular structures in the x plane.[11–13]

In our work we studied the phase transitions in compounds of the jarosite type. Since in such compounds the neighboring layers with Fe^{3+} are separated by nonmagnetic ions of S, O, K, and OH, layer-to-layer exchange is much smaller than the intraplanar exchange J_1. It has also been established that in some substances, e.g., with M=K, the spins in a layer are perpendicular to the c axis as a result of magnetic ordering.[12] Below we allow for the interaction between nearest-neighbor and next-nearest-neighbor spins on a Kagomé lattice separated by distances Δ_1 and Δ_2, respectively,

$$H=J_1\sum_{i\Delta_1}\mathbf{S}_i\cdot\mathbf{S}_{i+\Delta_1}+J_2\sum_{i\Delta_2}\mathbf{S}_i\cdot\mathbf{S}_{i+\Delta_2}, \tag{1}$$

and limit our study to systems with XY-like spins: $\mathbf{S}_i=S(\cos\theta_i,\sin\theta_i)$.

As for Ising systems with a Kagomé lattice, it is known[14] that phase transitions are possible only when next-nearest-neighbors interact antiferromagnetically $(J_2<0)$, but compounds with Ising spins have yet to be found. In contrast to such compounds, XY systems have continuous symmetry in

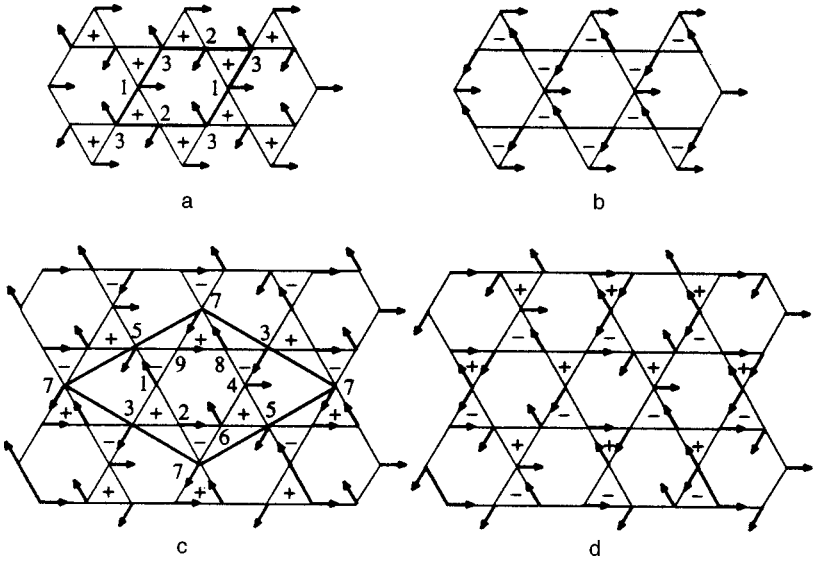

FIG. 1. Degenerate ground states for $j>0$ (a and b) and $j<0$ (c and d); the ''plus'' and ''minus'' indicate the sign of the parameter k on the elementary triangles. The heavy lines depict the unit magnetic cells with three (a) and nine (c) spins.

the plane. Further, in contrast to Heisenberg systems, they also have discrete symmetry, since at $T=0$ the chiral parameter specified for each elementary triangle,[15]

$$\mathbf{k}=\frac{2}{3\sqrt{3}}((\mathbf{S}_1\mathbf{S}_2)+(\mathbf{S}_2\mathbf{S}_3)+(\mathbf{S}_3\mathbf{S}_1)) \tag{2}$$

(the spins are numbered clockwise), takes a value of $+1$ or -1. The situation resembles triangular antiferromagnets with planar spins,[16,17] but here, first, the chiral parameter does not change sign for $J_2>0$ and, second, the unit cell on a Kagomé lattice has nine spins instead of three for $J_2<0$. We find that although for next-nearest-neighbor antiferromagnetic interaction ($J_2>0$) the ordering process is slower than that for ferromagnetic interaction ($J_2<0$), in both cases there exists a finite critical temperature at which translational spin and chiral orders emerge simultaneously.

2. THE LOW-TEMPERATURE RANGE

The ground state on a Kagomé lattice strongly depends on the sign of the exchange interaction J_2 between next-nearest-neighbors. For antiferromagnetic exchange, $J_2>0$, this state has a structure with three spins per unit cell (Fig. 1a), while for $J_2<0$ the structure consists of nine spins (Fig. 1c). In both cases the spin configurations are continuously degenerate with respect to rotations in the plane and are two-fold symmetric. For $J_2>0$ the discrete degeneracy is characterized by a k of fixed sign (Figs. 1a and 1b), while for $J_2<0$ the value of k changes sign in neighboring elementary triangles (Figs. 1c and 1d). A transition between two equivalent states amounts to surmounting an energy barrier proportional to $|J_2|$. We expect that in the low-temperature range the related excitations are suppressed and the system can be described in the harmonic approximation. Let us examine the properties of the phases at low temperatures for states with three and nine spins per unit magnetic cell.

In the state with three spins per unit cell, $J_2>0$, the Hamiltonian in the quadratic approximation in $\psi_k=(\psi_{k1},\psi_{k2},\psi_{k3})$ (here $\psi_{k\alpha}$ are the Fourier transforms of the deviation of the sublattice α from the equilibrium structure) can be written as

$$H=-(J_1+J_2)S^2N+\frac{1}{2}S^2\sum_k \psi_k M_k \psi_{-k}, \tag{3}$$

where the elements of the 3×3 matrix M_k are

$$\begin{aligned}
M_{11}&=M_{22}=M_{33}=2(J_1+J_2),\\
M_{12}&=M_{21}=-J_1\cos\left(\frac{k_x}{2}+\frac{\sqrt{3}}{2}k_y\right)\\
&\quad -J_2\cos\left(\frac{3}{2}k_x-\frac{\sqrt{3}}{2}k_y\right),\\
M_{23}&=M_{32}=-J_1\cos\left(\frac{k_x}{2}-\frac{\sqrt{3}}{2}k_y\right)\\
&\quad -J_2\cos\left(\frac{3}{2}k_x+\frac{\sqrt{3}}{2}k_y\right),\\
M_{31}&=M_{13}=-J_1\cos k_x-J_2\cos\sqrt{3}k_y.
\end{aligned} \tag{4}$$

When k is small, for the smallest eigenvalue of the matrix M_k we obtain

$$\lambda_1=\frac{1}{2}(J_1+3J_2)k^2 \tag{5}$$

($\lambda_2=\lambda_3\simeq3(J_1+J_2)$). In the low-temperature range we have the following expressions for the energy $E=\langle H\rangle$, the spin–spin correlation function, and the chiral parameter $k(T)$:

$$E=-(J_1+J_2)S^2N\left[1-\frac{T}{2(J_1+J_2)S^2}\right], \tag{6}$$

$$\langle\mathbf{S}_o\cdot\mathbf{S}_r\rangle=\exp\left[-\frac{\langle(\psi_o-\psi_r)^2\rangle}{2}\right]\sim r^{-\eta(T)}, \tag{7}$$

where o and r belong to the same sublattice,

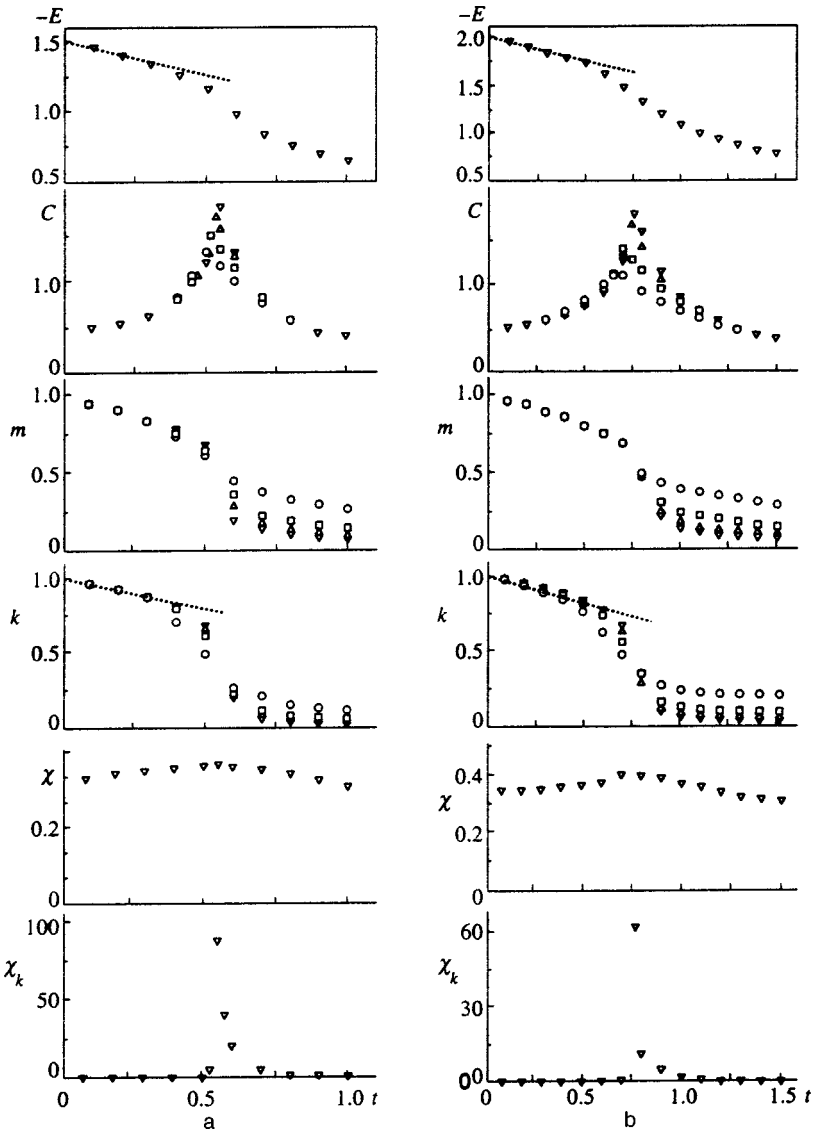

FIG. 2. Energy, heat capacity, magnetization, chiral parameter, and susceptibilities χ and χ_k versus the normalized temperature $t=T/J_1S^2$ at $j=0.5$ (a) and $j=-0.5$ (b). The symbols ○, □, △, and ▽ correspond to $L=12$, 24, 36, and 48.

$$\eta(T)=\frac{T}{\pi(J_1+3J_2)S^2}, \tag{8}$$

$$k(T)=\frac{1}{N}\left\langle \sum_R k(R)\right\rangle = 1-\frac{T}{2(J_1+3J_2)S^2} \tag{9}$$

(R stands for the coordinates of the points of the dual lattice).

In the states with nine spins per unit cell, $J_2<0$, the smallest eigenvalue of M_k, the spin–spin correlation function, and the chiral parameter $k(T)$ in the low-temperature range are given by the same expressions (5)–(9) but with $-2J_2$ substituted for J_2.

The process of ordering of planar spins on a Kagomé lattice was studied for arbitrary T by the Monte Carlo method. In comparison to a triangular lattice, the number of spins on a Kagomé lattice is smaller by 1/4, or $N=3L^2/4$, where L in our calculations varied from 12 to 48. The heat capacity and the magnetic susceptibility were found by numerical calculations from the fluctuations of the energy and magnetization, respectively. We also calculated the mean square of the sublattice magnetization:

$$m^2=\frac{1}{N_\alpha}\left\langle \sum_{N_\alpha} M_\alpha^2\right\rangle \tag{10}$$

($N_\alpha=3$ for $J_2>0$ and $N_\alpha=9$ for $J_2<0$; M_α is the sublattice magnetization), the parameter $k(T)$, and the corresponding susceptibility χ_k.

The temperature dependence of the thermodynamic quantities for $j=\pm 0.5$ ($j=J_2/J_1$) is depicted in Fig. 2. At low temperatures the behavior of the energy can be described by the harmonic approximation (6) for $j=0.5$ and by the same expression with $-2J_2$ substituted for J_2 in (6) for $j=-0.5$. Deviations from the linear dependence emerge for $T/J_1S^2>0.3$ in Fig. 2a and for $T/J_1S^2>0.5$ in Fig. 2b. The parameter $k(T)$ behaves in the linear region in a similar way, in accordance with the expected relationships of type (9).

The exponent $\eta(T)$ for the spin–spin correlation function can be determined from the dimensional relationship

$$m^2\sim L^{-\eta(T)}. \tag{11}$$

We calculated the parameter $\eta(T)$ from the slope of the asymptotic straight lines for $-\ln m^2$ as a function of $\ln L$.

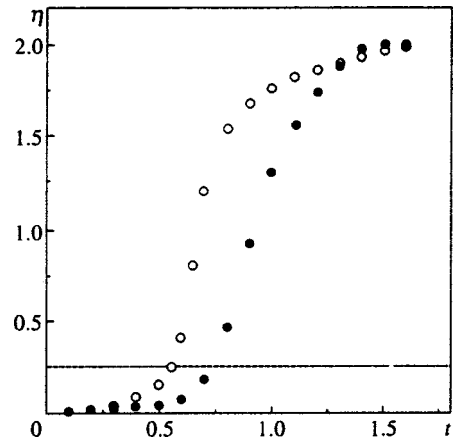

FIG. 3. Temperature dependence of η. The symbols ○ and ● correspond to diagrams with $j=0.5$ and $j=-0.5$, respectively.

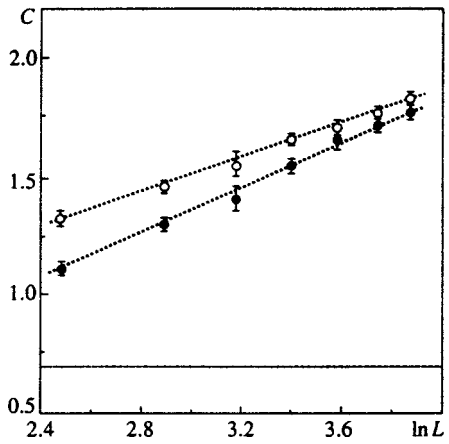

FIG. 4. The maximum in heat capacity as a function of ln L. The symbols ○ and ● correspond to the same values of j as in Fig. 3.

The results for different values of T are depicted in Fig. 3. As the temperature increases, deviations from the linear dependence emerge at the same values of T as for the internal energy.

3. PHASE TRANSITION

The appreciable difference between the antiferromagnetic systems with $J_2=0$ and $J_2\neq 0$ manifests itself in the behavior of the heat capacity and the susceptibilities (Fig. 2). For instance, when we have $J_2\neq 0$, the heat capacity and the chiral susceptibility have a peak that increases with lattice size and becomes sharper, while the homogeneous susceptibility χ has a broad maximum in a specific temperature range. The dimensional dependence of the height of the heat-capacity peak is depicted in Fig. 4: obviously, the logarithmic divergence is due to a phase transition in the parameter k.

We expect that in the limit $N\to\infty$ the behavior of k is described by the following formula:

$$k^2N=[k(N\to\infty)]^2N+O(N). \tag{12}$$

The dimensional dependence of k^2N on N at $j=\pm 0.5$ is depicted in Figs. 5a and 5b. The values of $k(T)$ for an infinite system were calculated from the slope of the asymptotic straight lines (dotted lines). On the basis of these data, we constructed (Figs. 5c and 5d) the dependence of $-\ln k$ on

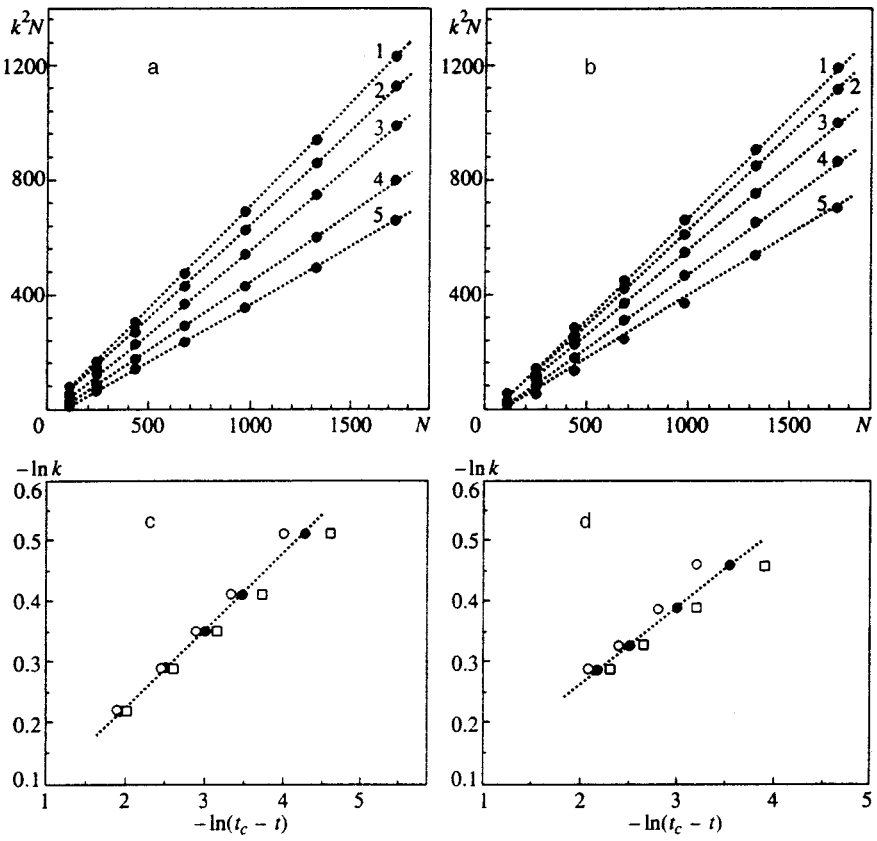

FIG. 5. (a,b)—Dimensional dependence of k^2N at different temperatures. The slopes of the asymptotic straight lines (dotted lines) yield the value of k^2 for an infinite system. The straight lines *1–5* correspond to $t=0.36$, 0.41, 0.46, 0.51, and 0.53 at $j=0.5$ (a) and $t=0.52$, 0.57, 0.62, 0.67, and 0.72 at $j=-0.5$ (b). (c,d)—The parameter k extrapolated to an infinite system as a function of the normalized temperature t (log–log scale) at $j=0.5$ (c) and $j=-0.5$ (d). The symbols ○, ●, and □ correspond to $t_c=0.55$, 0.54, and 0.53 at $j=0.5$ (c) and $t_c=0.74$, 0.73, and 0.72 at $j=-0.5$ (d). The dotted lines have a slope $\beta=0.12\pm 0.01$.

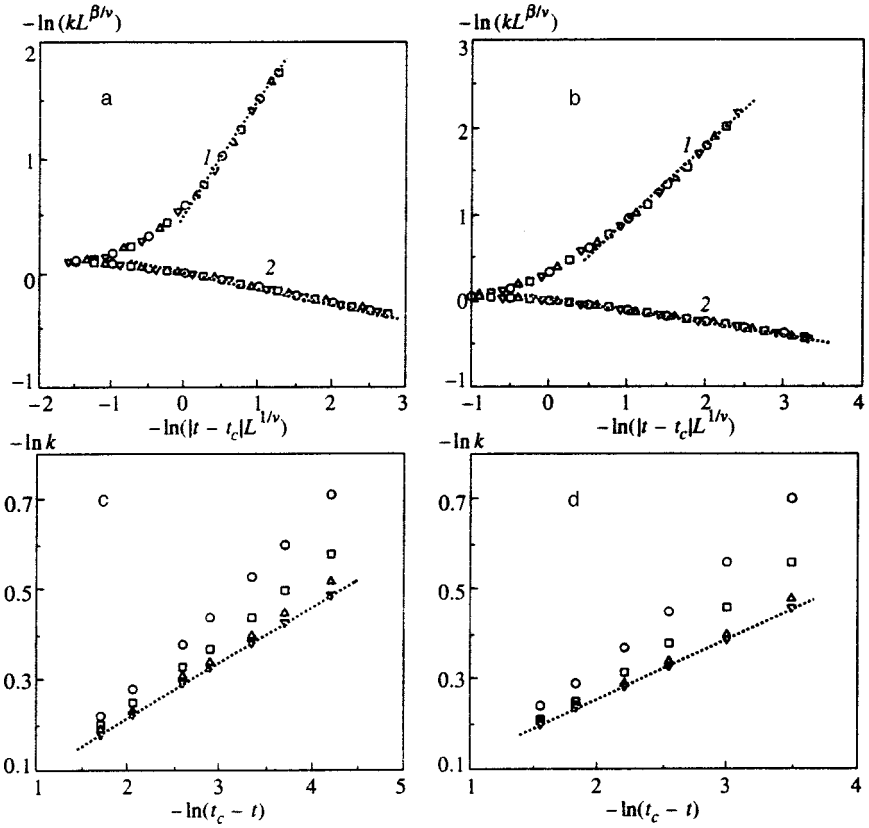

FIG. 6. (a,b)—The scaling functions for the parameter k above and below T_c (curves *1* and *2*, respectively) at $j=0.5$ (a) and $j=-0.5$ (b). The symbols ○, □, △, and ▽ correspond to $L=12$, 24, 36, and 48. The dotted straight lines have a slope $\nu-\beta=7/8$ for $T>T_c$ and $-\beta=-1/8$ for $T<T_c$. (c,d)—The temperature dependence of the parameter k for finite-size systems (log–log scale); $t_c=0.535$ at $j=0.5$ (c) and $t_c=0.726$ at $j=-0.5$ (d). The symbols ○, □, △, and ▽ correspond to $L=12$, 24, 36, and 48. The dotted straight lines have a slope $\beta=1/8$.

$-\ln(t_c-t)$ for different trial values of $t_c(=T_c/J_1S^2)$. The critical temperature t_c is found under the assumption that the chiral parameter is a power function: $k(t)\sim(t-t_c)^{\beta}$. Figures 5c and 5d show that for any sign of j a straight line with a slope $\beta=0.12\pm0.01$ emerges at $t_c=0.54\pm0.01$ for $j=0.5$ and at $t_c=0.73\pm0.01$ for $j=-0.5$.

We also did a finite-size-scaling analysis under the assumption that

$$kL^{\beta/\nu}=F_k(|t-t_c|L^{1/\nu}), \tag{13}$$

where F_k is the scaling function.[18] Below t_c the relationship (13) reduces to $k\sim(t_c-t)^{\beta}$ in the limit $L\to\infty$, so that for F_k we have

$$F_k\sim x^{\beta} \tag{14}$$

as $x\to\infty$. On the other hand, above t_c the parameter k is proportional to $1/\sqrt{N}\sim 1/L$, so that in this case

$$F_k(x)\sim x^{\beta-\nu} \tag{15}$$

as $x\to\infty$. The best values of t_c, β, and ν, obtained from the conditions that the data for different lattice sizes lie on a single curve (Figs. 6a and 6b) and the limiting relations (14) and (15) are valid, are as follows: $t_c=0.535$ at $j=0.5$ and $t_c=0.726$ at $j=-0.5$, and $\beta=1/8$ and $\nu=1$ irrespective of the sign of j. We see that the calculated values of the transition temperatures and the critical exponents in Figs. 6a and 6b are in good agreement with the similar calculated values in Figs. 5c and 5d.

For these values $t_c=0.535$ ($j=0.5$) and $t_c=0.726$ ($j=-0.5$) we have also found the $-\ln k$ vs. $-\ln(t_c-t)$ dependence for different values of L (Figs. 6c and 6d). Near the transition temperature the data of the numerical calculations deviate from a straight line (the dotted line) because of the finiteness of L. In the region where the data for different lattice sizes lie on a common straight line, the lines correspond to the slope $\beta=1/8$ (as in the previous calculations).

Above T_c, scaling analysis of the chiral susceptibility χ_k was done on the basis of the following relationship:

$$t\chi_kL^{-\gamma/\nu}=F_{\chi}(|t-t_c|L^{1/\nu}). \tag{16}$$

Obviously, as $x\to\infty$, the scaling function $F_{\chi}(x)$ assumes the following form:

$$F_{\chi}(x)\sim x^{-\gamma}\ (t>t_c), \tag{17}$$

since in the thermodynamic limit $L\to\infty$ we must have $t\chi_k\sim|t-t_c|^{-\gamma}$. The values of γ and ν were chosen from the conditions that the numerical data for lattices with different Ls lie on the same curve and that the limit (17) holds. The best coincidence at $t_c=0.535$ for the case $j=0.5$ and at $t_c=0.726$ for the case $j=-0.5$ was obtained with $\nu=1$ and $\gamma=7/4$ (Figs. 7a and 7b).

Thus, the foregoing results show that, irrespective of the sign of j (and hence of the number of spins per unit cell), the critical behavior in a phase transition is described by the critical exponents of two-dimensional Ising systems. This fact is not accidental and is due to the symmetry of the systems with respect to sign reversal of k.

In determining the temperature of the Berezinskii–Kosterlitz–Thouless transition it is convenient to study the correlation function

$$g(r)=\langle\cos 3(\psi_0-\psi_r)\rangle\sim r^{-9\eta_{xy}(T)}, \tag{18}$$

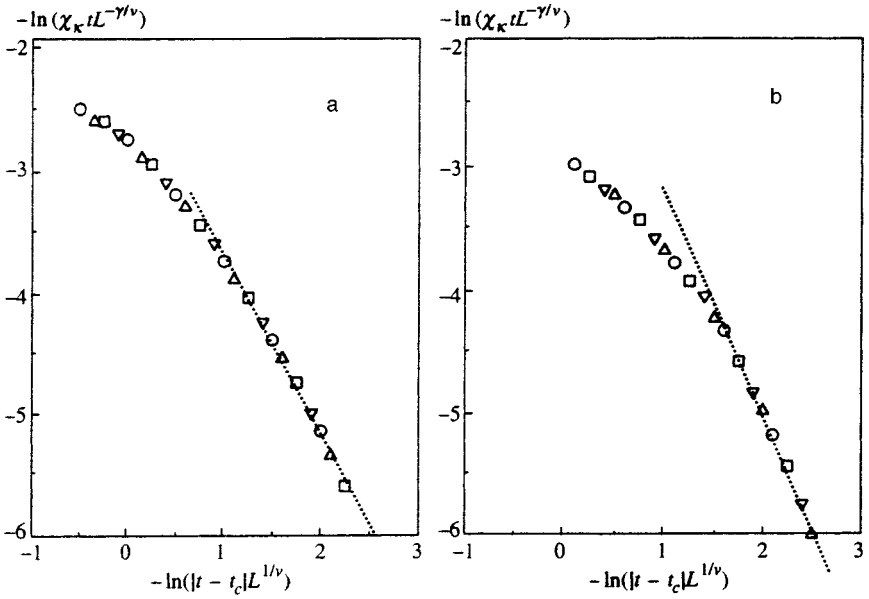

FIG. 7. The scaling functions for the chiral susceptibility above T_c at $j=0.5$ (a) and $j=-0.5$ (b). The symbols ○, □, △, and ▽ correspond to $L=12$, 24, 36, and 48. The dotted straight lines have a slope $-\gamma=-7/4$.

which makes it possible to isolate the contribution of continuous fluctuations at T below the temperature of the Ising transition and to correctly determine the phase transition if it occurs at temperature higher than that for the transition in discrete variables. Figure 8 depicts the power-function behavior of $g(r)$ for $j=\pm 0.5$ at different temperatures. Using the Berezinskii–Kosterlitz–Thouless criterion $\eta_{xy}(T_{\mathrm{BKT}})=1/4$, we found that the phase transition with continuous-symmetry breaking occurs at $t_{\mathrm{BKT}}=0.542\pm 0.003$ at $j=0.5$ and $t_{\mathrm{BKT}}=0.733\pm 0.003$ at $j=-0.5$, where $t_{\mathrm{BKT}}=T_{\mathrm{BKT}}/JS^2$. Within the accuracy of the calculations, t_{BKT} coincides with t_c, so that a phase transition in the system is realized at a single temperature, irrespective of the sign of $j(=\pm 0.5)$. Note that, to the accuracy of calculations, the behavior of η in (8) yields the same value of t_{BKT}. In this case for $\eta=1/4$ we have $t_{\mathrm{BKT}}=0.537\pm 0.002$ at $j=0.5$ and $t_{\mathrm{BKT}}=0.729\pm 0.003$ at $j=-0.5$. Similar calculations for other values of j that are not too close to zero show that both transitions occur simultaneously. The t_c-j phase diagram is depicted in Fig. 9. The neighborhood of the point $j=0$ where the two phase transitions may be expected to occur is probably very small and requires more exact calculations and extensive computer time.

In $KFe_3(OH)_6(SO_4)$, the magnetic susceptibility has a broad maximum at $T_c=60$ K (Ref. 10); the exchange interactions J_1 and J_2 are antiferromagnetic, with J_2 known to be smaller than J_1 by a factor of ten. At $j=0.1$ we have $t_c=0.22$. Thus, the exchange interaction between the nearest-neighbor Fe^{3+} ions with spins $S=5/2$ can be expected to be 44 K.

4. CONCLUSION

We have studied the magnetic properties of planar antiferromagnetic systems with a Kagomé lattice. We have found that with allowance for exchange interactions between next-nearest-neighbor spins there is a phase transition in the system at finite temperatures. In the low-temperature phase there is long-range order in the parameter k, and the correlation function decreases according to a power law. Scaling analysis of finite-size systems shows that k vanishes at the same temperature at which the chiral susceptibility diverges, and their behavior is described fairly well by the critical exponents of two-dimensional Ising systems. We have also found that the temperature of a Berezinskii–Kosterlitz–Thouless transition and the temperature of an Ising transition

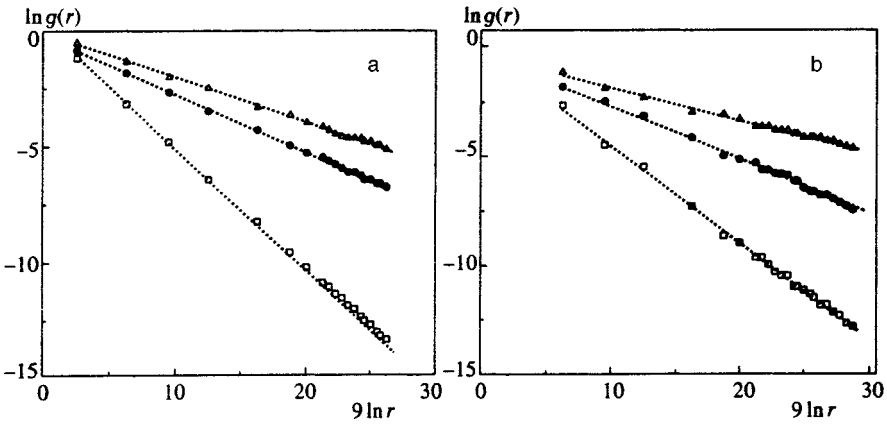

FIG. 8. Spatial dependence of the correlation function $g(r)$ for $L=48$. The symbols △, ●, and □ correspond to $t=0.519$, 0.542, and 0.565 and the slope of the dotted lines $\eta_{xy}=0.18$, 0.25, and 0.5 (a), and $t=0.664$, 0.733, and 0.804 and $\eta_{xy}=0.12$, 0.25, and 0.45 (b).

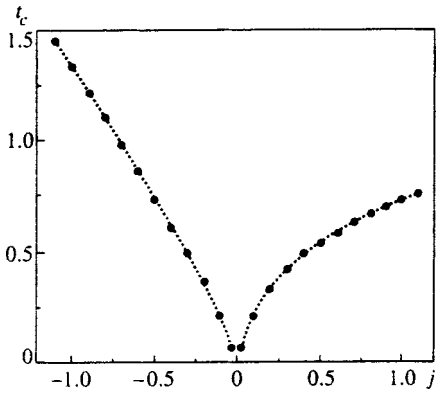

FIG. 9. The phase diagram in the $t_c - j$ plane for planar antiferromagnetic systems with a Kagomé lattice.

coincide to within the accuracy of the calculations. We expect that our result can be used for a detailed experimental study of jarosite-type compounds. Note that in real systems with weak interplanar interaction there is a narrow but finite temperature range where the critical behavior is three-dimensional. However, the vast body of experimental data suggests that, say, for the layered XY ferromagnet Rb_2CrCl_4 (Ref. 19), the Ising antiferromagnet K_2CoF_4 (Ref. 20), the triangular antiferromagnet VCl_2 (Ref. 21), and other magnetic materials (Ref. 22) the behavior outside this range is two-dimensional, although there is three-dimension long-range order in the system.

In conclusion we note that in Ising-like Heisenberg antiferromagnets, where due to distortions in the 120° structure there is a finite magnetic moment on each elementary triangle of the Kagomé lattice, a drop in temperature can lead to a phase transition with discrete- and continuous-symmetry breaking.[23] Therefore, we expect that the behavior of such systems is in many respects similar to the behavior of the planar (XY) antiferromagnetic systems considered in this paper.

This work was supported by the Krasnoyarsk Regional Scientific Fund (Project 6F0061).

*)E-mail: theor@iph.krasnoyarsk.su

[1] P. Chandra, P. Coleman, and I. Ritchey, J. Phys. (Paris) **33**, 591 (1993).
[2] J. T. Chalker, P. C. W. Holdsworth, and E. F. Shender, Phys. Rev. Lett. **68**, 855 (1992).
[3] A. B. Harris, C. Kallin, and A. J. Berlinsky, Phys. Rev. B **45**, 2899 (1992).
[4] A. Sütö, Z. Phys. B **44**, 121 (1981).
[5] R. S. Gekht and V. I. Ponomarev, Phase Transit. **20**, 27 (1990).
[6] C. Zeng and V. Elser, Phys. Rev. B **42**, 8436 (1990).
[7] A. Chubukov, Phys. Rev. Lett. **69**, 832 (1992).
[8] D. A. Huse and A. D. Rutenberg, Phys. Rev. B **45**, 7536 (1992).
[9] R. Wang, W. F. Bradley, and H. Steinfink, Acta Crystallogr. **18**, 249 (1965).
[10] A. Bonnin and A. Lecerf, C. R. Acad. Sci. **262**, 1782 (1966).
[11] M. G. Townsend, G. Longworth, and E. Roudaut, Phys. Rev. B **33**, 4919 (1986).
[12] M. Takano, T. Shinjo, and T. Takada, J. Phys. Soc. Jpn. **30**, 1049 (1971).
[13] A. Keren, K. Kojima, L. P. Le, G. M. Luke, W. D. Wu, Y. J. Uemura, M. Takano, H. Dabkowska, and M. J. P. Gingras, Phys. Rev. B **53**, 6451 (1996).
[14] T. Takagi and M. Mekata, J. Phys. Soc. Jpn. **62**, 3943 (1993).
[15] J. Villain, J. Phys. (France) **38**, 385 (1977).
[16] S. Miyashita and H. Shiba, J. Phys. Soc. Jpn. **53**, 1145 (1984).
[17] D. H. Lee, J. D. Joannopoulos, J. W. Negele, and D. P. Landau, Phys. Rev. B **33**, 450 (1986).
[18] *Finite Size Scaling and Numerical Simulation of Statistical Systems*, V. Privman (Ed.), World Scientific, Singapore (1990).
[19] S. T. Bramwell, P. C. W. Holdsworth, and M. T. Hutchings, J. Phys. Soc. Jpn. **64**, 3066 (1995).
[20] H. Ikeda and K. Hirakawa, Solid State Commun. **14**, 529 (1974).
[21] H. Kadowaki, K. Ubukoshi, K. Hirakawa *et al.*, J. Phys. Soc. Jpn. **56**, 4027 (1987).
[22] E. J. Samuelsen, Phys. Rev. Lett. **31**, 936 (1973).
[23] A. Kuroda and S. Miyashita, J. Phys. Soc. Jpn. **64**, 4509 (1995).

Translated by Eugene Yankovsky